The Design and Performance of Three-Line Microstrip Couplers

DIMITRIOS PAVLIDIS, STUDENT MEMBER, IEEE, AND HANS L. HARTNAGEL, SENIOR MEMBER, IEEE

Abstract—**An analysis is presented of microstrip-coupler circuits consisting of three parallel lines. The analysis is based on the existence of three mode impedances. Design equations describing the performance of this type of coupler are derived and allow the prediction of its matching and transmission properties. Numerical results using finite-difference methods are presented for a three-line microstrip coupler made on an alumina substrate (k = 9.8). Experimental results for a 10-dB three-line coupler with a center frequency of 4 GHz show that its performance can be reasonably well predicted by the developed theory.**

I. Introduction

COMMUNICATION SYSTEMS and other microwave applications often require the use of special coupler structures such as a three-line symmetrical coupler for combining two independent signals on to a common third line.

The properties of multiconductor networks have been examined extensively by many authors [1]–[6]. First results [1], [2] were limited primarily to the design of microwave interdigital filters. The geometry of these networks allows one to neglect the coupling capacitances beyond the nearest neighbor conductors. In this way wave propagation along the lines can be described by the use of two orthogonal TEM modes, namely the even and odd mode [1]–[3]. A more complete analysis taking into consideration the effect of the fringing capacitances beyond the nearest neighbors of an array of three conductors also exists [4], [5]. Yamamoto *et al.* [5] introduced three modes of propagation and five characteristic mode impedances, three of which are independent. In their theory the mode impedances of the center conductors are related to those of the side conductors by a special condition for the capacitance or potential coefficients of the structure. The theory developed in this paper makes no use of Yamamoto's condition, which was possible by making a suitable choice of the modes of propagation. These modes of propagation were excited in the conductors by using voltage and current sources whose amplitudes were tailored to the particular network geometry.

The fundamental modes of propagation for a network having three parallel conductors are derived in Section II of this paper. The coupling beyond nearest neighbors is included and the wave propagation is described by only three mode impedances. Section III describes the impedance-matrix derivations for an array of three lines of finite length excited by the method described in Section II. The relations predicting the performance of such a network when used as a coupler are derived in Section IV. The method used for the calculation of the mode impedances is outlined in Section V. Mode-impedance data are presented in Section VI and are valid for couplers made on alumina substrates of a relative dielectric constant k = 9.8. Finally, Section VII describes experimental results obtained with a construction of a three-line coupler which is designed in accordance with the developed theory. Such a type of coupler has been successfully used for combining the signals of two pulsed Gunn oscillators employed in the phase-shift-keyed (PSK) X-band modulator of [7] and [8].

Manuscript received August 11, 1975; revised March 31, 1976.

The authors are with the Department of Electrical and Electronic Engineering, University of Newcastle upon Tyne, Newcastle upon Tyne, England.

II. Derivation of the Fundamental Modes of Propagation

Every TEM propagation along a set of three parallel lines having a fourth line as a common earth can be described by the use of three fundamental eigenvectors which are orthogonal to each other [9]. The assumption of a TEM mode had to be made for the following derivations because of the resulting relatively simple approach to the problem. No pure TEM transmission can, of course, exist in a microstrip circuit, like the one which will be explored in the later parts of this paper, because of its nonhomogeneous nature.

In order to derive the fundamental modes of propagation, it is necessary to assume three infinite long parallel lines. If wave propagation takes place in the y direction, then we can write, according to conventional transmission-line theory,

$$\frac{d[V]}{dy} = -[z][I]. \tag{II.1}$$

In the previous equation the elements V_i and I_i, (i = 1,2,3) of the matrices $[V]$ and $[I]$ denote the voltage and current at the port i of the network and $[z]$ is the square 3 × 3 matrix of the impedance coefficients z_{ij}, (i,j = 1,2,3). From symmetry considerations we have, of course,

$$[z] = \begin{bmatrix} z_{11} & z_{12} & z_{13} \\ z_{12} & z_{22} & z_{12} \\ z_{13} & z_{12} & z_{11} \end{bmatrix} \qquad [V] = \begin{bmatrix} V_1 \\ V_2 \\ V_3 \end{bmatrix} \qquad [I] = \begin{bmatrix} I_1 \\ I_2 \\ I_3 \end{bmatrix}. \tag{II.2}$$

The eigenvalue equation for the impedance matrice $[z]$ is

$$([z] - \lambda[E])[x] = 0 \tag{II.3}$$

where $[x]$ is a matrix with columns denoting the eigenvectors of $[z]$, $[E]$ is the unity matrix, and $[\lambda] = \lambda[E]$ is a matrix whose diagonal elements are the eigenvalues of

$[z]$. Equation (II.3) results in a third-order equation which has the following solutions:

$$\lambda_1 = z_{11} - z_{13} \tag{II.4}$$

$$\lambda_2 = [z_{11} + z_{22} + z_{13} + \sqrt{(z_{11} - z_{22} + z_{13})^2 + 8z_{12}^2}]/2 \tag{II.5}$$

and

$$\lambda_3 = [z_{11} + z_{22} + z_{13} - \sqrt{(z_{11} - z_{22} + z_{13})^2 + 8z_{12}^2}]/2. \tag{II.6}$$

The eigenvector x_a corresponding to the eigenvalue λ_1 can be easily calculated by introducing (II.4) into (II.3)

$$x_a = k \begin{bmatrix} -1 \\ 0 \\ 1 \end{bmatrix} = \begin{bmatrix} x_{a1} \\ x_{a2} \\ x_{a3} \end{bmatrix} \tag{II.7}$$

where k is some arbitrary value of x_{a1}.

A more laborious calculation gives for the remaining two eigenvectors

$$x_b = k \begin{bmatrix} 1 \\ \eta_1 \\ 1 \end{bmatrix} = \begin{bmatrix} x_{b1} \\ x_{b2} \\ x_{b3} \end{bmatrix} \tag{II.8}$$

and

$$x_c = k \begin{bmatrix} 1 \\ \eta_2 \\ 1 \end{bmatrix} = \begin{bmatrix} x_{c1} \\ x_{c2} \\ x_{c3} \end{bmatrix} \tag{II.9}$$

where

$$\eta_1 = \frac{-K + L + M}{K + L + N} \frac{z_{12}}{z_{13}} \tag{II.10}$$

$$\eta_2 = \frac{-K - L + M}{K - L + N} \frac{z_{12}}{z_{13}} \tag{II.11}$$

$$K = z_{11} - z_{22} \qquad L = [(z_{11} - z_{22} + z_{13})^2 + 8z_{12}^2]^{1/2}$$

$$M = 3z_{13} \qquad N = z_{13} + \frac{2z_{12}^2}{z_{13}} \tag{II.12}$$

and k is the arbitrary value of x_{b1} and x_{c1}.

It can be easily shown that the following simple relation holds between η_1 and η_2 for any value of z_{ij}:

$$\eta_1 \eta_2 = -2. \tag{II.13}$$

Equation (II.13) shows that by assigning a value μ to η_1, it is always possible to express η_2 as

$$\eta_2 = -2/\mu. \tag{II.14}$$

From the eigenvectors x_a, x_b, and x_c we can now derive the following conditions for each of the three possible voltage modes:

$$OE\text{-mode} \quad V_a = -V_c, \; V_b = 0 \tag{II.15}$$

$$EE\text{-mode} \quad V_a = V_c = \frac{V_b}{\mu} \tag{II.16}$$

$$OO\text{-mode} \quad V_a = V_c = -\frac{\mu}{2} V_b \tag{II.17}$$

$$\mu = \frac{-K + L + M}{K + L + N} \frac{z_{12}}{z_{13}} \tag{II.18}$$

where V_a, V_b, and V_c are the voltages exciting the lines, a, b, and c, respectively. In accordance with the aforementioned notation of the voltage modes, the eigenvalues (II.4)–(II.6) will in the following be referred to as mode impedances Z_{oe}, Z_{ee}, and Z_{oo}, respectively.

It will now be shown for a network which is excited according to (II.15)–(II.17) that the characteristic impedance of the center conductor will always be the same as that of the side conductor; this implies that it is not necessary to impose any condition for the capacitance coefficients of the network (as used, for example, by [5]). The OE mode of our theory is the same as the C mode of [5], but the EE and OO modes are different by the factors $1/\mu$ and $\mu/2$, respectively. The parameter μ is an internal property of each particular network. As μ changes, with the geometry of the network, the value of the characteristic impedance of the center conductor is automatically adjusted to that of the side conductors. By using the same method as [5] we obtain the following expressions for the static capacitances to ground per unit length of each conductor:

$$OE\text{-mode} \quad C_{aoe} = C_{coe} = c_{11} - c_{13} \tag{II.19}$$

$$EE\text{-mode} \quad C_{aee} = C_{cee} = c_{11} + \mu c_{12} + c_{13}$$

$$C_{bee} = c_{22} + \frac{2}{\mu} c_{12} \tag{II.20}$$

$$OO\text{-mode} \quad C_{aoo} = C_{coo} = c_{11} - \frac{2}{\mu} c_{12} + c_{13}$$

$$C_{boo} = c_{22} - \mu c_{12} \tag{II.21}$$

where c_{ij}, $(i,j = 1,2,3)$ are the capacitance coefficients of the network. In order to have equal mode impedances for the center and side conductors, we need

$$C_{aee} = C_{bee} = C_{cee}$$

$$C_{aoo} = C_{boo} = C_{coo} \tag{II.22}$$

or

$$\mu = \frac{-(c_{11} - c_{22} + c_{13}) - \sqrt{(c_{11} - c_{22} + c_{13})^2 + 8c_{12}^2}}{2c_{12}}. \tag{II.22a}$$

The condition expressed by (II.22a) is, in fact, always true because it is equivalent to (II.18), which is the fundamental parameter employed for the definition of the voltage modes. The equivalence of (II.22a) and (II.18) has been checked by numerical substitutions of the results obtained in Section VI; the values of μ calculated in this way were in both cases the same.

As (II.22a) is always valid, it is a matter of algebraic calculations to show in the same way as [5] that the following conditions apply for a network excited according to (II-15)–(II.17):

$$OE\text{-mode} \quad Q_a = Q_c, \; Q_b = 0 \tag{II.23}$$

$$EE\text{-mode} \quad Q_a = Q_c = Q_b/\mu \tag{II.24}$$

$$OO\text{-mode} \quad Q_a = Q_c = -\frac{\mu}{2} Q_b \tag{II.25}$$

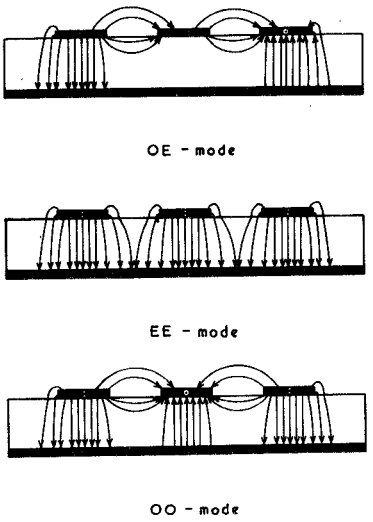

Fig. 1. Sketch of the electric-field lines for the fundamental modes existing in a three-line microstrip coupler.

where Q denotes the charge per unit length of each conductor.

Fig. 1 is a sketch of the electric-field lines for the three fundamental modes existing in an array of three parallel lines excited by equal magnitude voltages but having the phase relation implied by (II.15)–(II.17).

III. Impedance Matrix

The fundamental modes derived in Section II can be used for the evaluation of the impedance matrix of a three-line coupler. The method of calculation is based on the analysis presented in the classic paper by Jones and Bolljahn [10].

The $[Z]$ matrix is obviously expected to be a square matrix of order six since it refers to a coupler with three lines of length l, which is a six-port network. Each fundamental mode is excited by ideal current generators placed at the ends of the coupled transmission lines and having a certain phase and magnitude relation between them (Fig. 2). Under the aforementioned conditions, the electromagnetic coupling occurs over a finite length l and the total terminal voltages and currents can be derived by superimposing the corresponding values of voltage and current for each of the *OE*, *EE*, and *OO* types of excitation.

The current generators of Fig. 2 have the following values:

$$i'_{1ee} = \mu i_{1ee} \qquad i'_{2ee} = \mu i_{2ee}$$
$$i''_{1oo} = \frac{2}{\mu} i_{1oo} \qquad i''_{2oo} = \frac{2}{\mu} i_{2oo}. \tag{III.1}$$

The voltages $\mathfrak{V}$ produced by the employed current sources can now be easily expressed as a function of the position z along the line and of the corresponding mode impedance and current amplitude; in view of brevity the values of $\mathfrak{V}$ are presented for the *OE* mode only

$$\mathfrak{V}^{(a)}_{1oe} = -\mathfrak{V}^{(c)}_{1oe} = -jZ_{oe}i_{1oe}\frac{\cos k(l-z)}{\sin kl}$$
$$\mathfrak{V}^{(a)}_{2oe} = -\mathfrak{V}^{(c)}_{2oe} = -jZ_{oe}i_{2oe}\frac{\cos kz}{\sin kl}$$
$$\mathfrak{V}^{(b)}_{1oe} = \mathfrak{V}^{(b)}_{2oe} = 0. \tag{III.2}$$

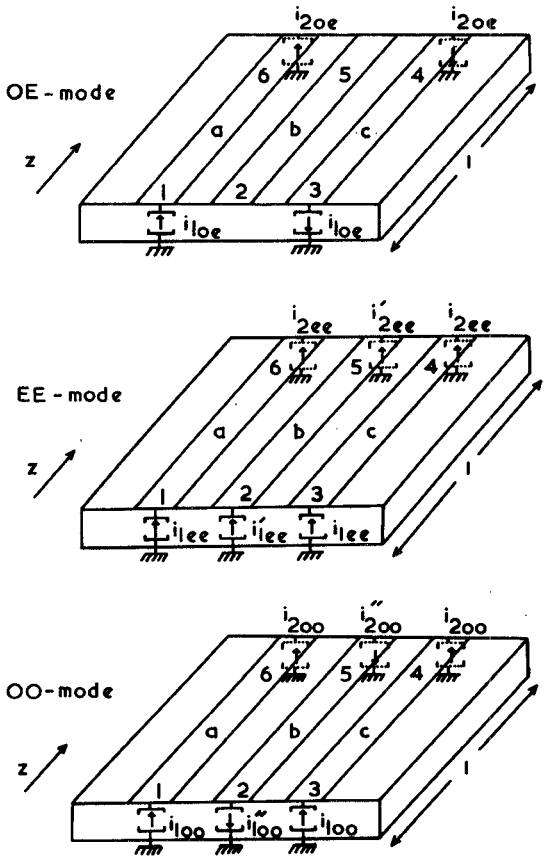

Fig. 2. Excitation of the fundamental modes of a three-line microstrip coupler by suitable current generators placed at its ports.

The total currents I_m, $(m = 1,\cdots,6)$ at each port can be expressed as a superposition of the mode currents i_{ij}, $(i = 1,2$, and $j = oe,ee,oo)$ resulting in six equations, the solution of which gives the values of i_{ij} in terms of I_m.

Similarly, by superimposing the mode voltages $\mathfrak{V}$ and introducing the $i_{ij}(I_m)$ values into (III.2) as well as into the corresponding equations which hold for the other two modes, the total voltages V_m can be expressed in the form $V_m = \sum_{n=1}^{6} Z_{mn}I_n$.

The coefficients Z_{mn} can thus be evaluated from the mode impedances Z_{oe}, Z_{oo}, and Z_{ee} and the electrical lengths $\theta = kl$. The elements of the impedance matrix $[Z]$ are given in Table I. A different phase velocity has been assumed for each of the three possible modes, and therefore the $[Z]$ matrix contains three different electrical lengths θ_{oe}, θ_{ee}, and θ_{oo}.

IV. Theoretical Prediction of the Performance of a Three-Line Coupler

An attempt is made here to express the properties of a three-line coupler, such as coupling coefficients, isolation, and matching in terms of the mode impedances Z_{oe}, Z_{ee}, and Z_{oo}. This will enable the designer to predict theoretically the desired performance of the coupler for each particular application.

The major difficulty in the analysis here is the expression of μ in (II.18) in terms of the mode impedances only. It can be seen from (II.18) that the value of μ depends on the geometrical configuration of the employed coupler. Every

analysis will therefore lose its generality by assuming some arbitrary μ, and thus simplifying the equations for the orthogonal eigenvectors (II.7)–(II.9). An analytical expression of μ in the form of $\mu = \mu(Z_{oe},Z_{ee},Z_{oo})$ could, however, not be derived because it is mathematically impossible to express all the $z_{11},z_{22},z_{12},z_{13}$ impedance coefficients of (II.4)–(II.6) in terms of Z_{oe}, Z_{ee}, and Z_{oo} only. One of the possible approaches to the problem is to express μ as $\mu(Z_{oe},Z_{ee},Z_{oo},z_{12})$, and then find the set of mode impedances which satisfies the desired performance for some arbitrary value of z_{12}; the design procedure becomes, however, in such a case very complicated, because there is a need for some optimization routine which can calculate a realistic set of values for Z_{oe}, Z_{ee}, Z_{oo}, and z_{12}, and reject all the nonrealistic solutions.

Another alternative is, of course, to reduce the z_{ij} coefficients by one, by making some reasonable assumption such as

$$z_{11} = z_{22}. \tag{IV.1}$$

The previous assumption can also be written in the following form:

$$c_{22} = c_{11} - \frac{c_{11}c_{12}}{c_{11} + c_{12} + c_{13}} + \frac{c_{11}c_{13}}{c_{11} + c_{12} + c_{13}} \tag{IV.1a}$$

where the c_{ij} are the capacitance coefficients introduced in Section II. By neglecting the coupling beyond the nearest neighbor conductor ($c_{13} = 0$), (IV.1a) reduces to the approximation expressed by [3, eq. (7)].

The impedance coefficients z_{ij} can now be written as

$$z_{11} = z_{22} = \tfrac{1}{3}(Z_{ee} + Z_{oo} + Z_{oe}) \tag{IV.2}$$

$$z_{13} = \tfrac{1}{3}(Z_{ee} + Z_{oo} - 2Z_{oe}) \tag{IV.3}$$

$$z_{12} = \frac{1}{\sqrt{18}}[2(Z_{ee} - Z_{oo})^2 - Z_{oe} \cdot (Z_{oe} - Z_{ee} - Z_{oo}) - Z_{ee}Z_{oo}]. \tag{IV.4}$$

It can be easily shown that μ is now given by

$$\mu = \sqrt{2}\,\frac{[2(Z_{ee} - Z_{oo})^2 - Z_{oe}(Z_{oe} - Z_{ee} - Z_{oo}) - Z_{ee}Z_{oo}]^{1/2}}{2Z_{ee} - Z_{oe} - Z_{oo}}. \tag{IV.5}$$

The validity of the assumption (IV.1) has been checked using the results of the numerical analysis which will be described in Section V of this paper. The values of z_{11} and z_{22} have been compared for a large number of possible geometrical configurations of the coupler and their difference never exceeded 2.5 percent; similarly, the value of μ given by (IV.5) is different from the correct value by not more than 4.6 percent.

For communication applications it is often required [7], [8] to have a three-line coupler with the following characteristics:

1) a perfectly matched input side port;
2) perfect isolation (decoupling) of the input side port from the side port which is at the same end of the lines [for example, ports 1 and 3 of Fig. 3(b)].

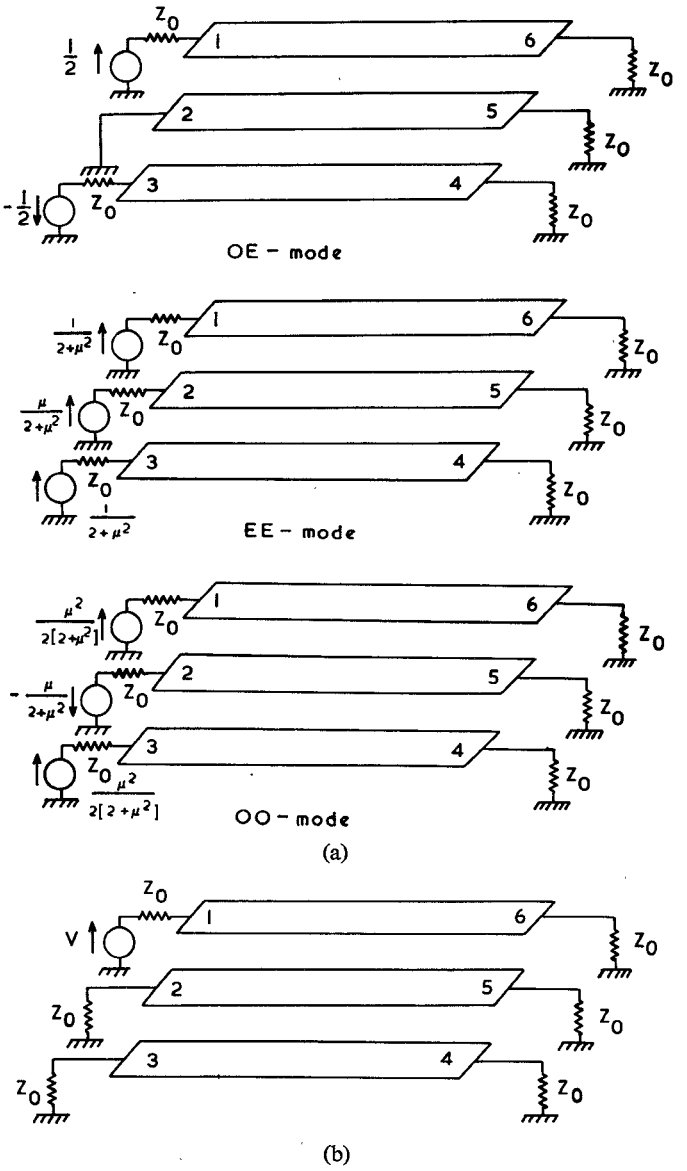

Fig. 3. (a) Sets of voltage sources required to excite the fundamental modes of a three-line coupler. (b) Driving of a three-line coupler by a voltage source.

The implications of the previous two conditions will now be examined. The scattering matrix of a symmetric six-port network consisting of three parallel conductors [Fig. 3(b)] can be written as

$$[S] = \left[\begin{array}{c|c} S^1 & S^2 \\ \hline S^2 & S^1 \end{array}\right] \tag{IV.6}$$

where

$$[S^1] = \begin{bmatrix} \alpha & \beta & \gamma \\ \beta & \theta & \beta \\ \gamma & \beta & \alpha \end{bmatrix}$$

and

$$[S^2] = \begin{bmatrix} \delta & \varepsilon & J \\ \varepsilon & \eta & \varepsilon \\ J & \varepsilon & \delta \end{bmatrix}. \tag{IV.7}$$

TABLE I
THE ELEMENTS OF THE IMPEDANCE MATRIX OF A THREE-LINE COUPLER

$$Z_{11} = Z_{33} = Z_{44} = Z_{66} = -j\left[\frac{Z_{oe}}{2}\cot\theta_{oe} + \frac{Z_{ee}}{2+\mu^2}\cot\theta_{ee} + \frac{\mu^2 Z_{oo}}{2(2+\mu^2)}\cot\theta_{oo}\right]$$

$$Z_{12} = Z_{21} = Z_{23} = Z_{32} = Z_{45} = Z_{54} = Z_{56} = Z_{65} = -j\left[\frac{\mu Z_{ee}}{2+\mu^2}\cot\theta_{ee} - \frac{\mu Z_{oo}}{2+\mu^2}\cot\theta_{oo}\right]$$

$$Z_{13} = Z_{31} = Z_{46} = Z_{64} = -j\left[-\frac{Z_{oe}}{2}\cot\theta_{oe} + \frac{Z_{ee}}{2+\mu^2}\cot\theta_{ee} + \frac{\mu^2 Z_{oo}}{2(2+\mu^2)}\cot\theta_{oo}\right]$$

$$Z_{14} = Z_{41} = Z_{36} = Z_{63} = -j\left[-\frac{Z_{oe}}{2}\frac{1}{\sin\theta_{oe}} + \frac{Z_{ee}}{2+\mu^2}\frac{1}{\sin\theta_{ee}} + \frac{\mu^2 Z_{oo}}{2(2+\mu^2)}\frac{1}{\sin\theta_{oo}}\right]$$

$$Z_{15} = Z_{51} = Z_{24} = Z_{42} = Z_{26} = Z_{62} = Z_{35} = Z_{53} = -j\left[\frac{\mu Z_{ee}}{2+\mu^2}\frac{1}{\sin\theta_{ee}} - \frac{\mu Z_{oo}}{2+\mu^2}\frac{1}{\sin\theta_{oo}}\right]$$

$$Z_{16} = Z_{61} = Z_{34} = Z_{43} = -j\left[\frac{Z_{oe}}{2}\frac{1}{\sin\theta_{oe}} + \frac{Z_{ee}}{2+\mu^2}\frac{1}{\sin\theta_{ee}} + \frac{\mu^2 Z_{oo}}{2(2+\mu^2)}\frac{1}{\sin\theta_{oo}}\right]$$

$$Z_{22} = Z_{55} = -j\left[\frac{\mu^2 Z_{ee}}{2+\mu^2}\cot\theta_{ee} + \frac{2Z_{oo}}{2+\mu^2}\cot\theta_{oo}\right]$$

$$Z_{25} = Z_{52} = -j\left[\frac{\mu^2 Z_{ee}}{2+\mu^2}\frac{1}{\sin\theta_{ee}} + \frac{2Z_{oo}}{2+\mu^2}\frac{1}{\sin\theta_{oo}}\right]$$

By applying the unitary property of $[S]$, it is possible to show that if $\alpha = \gamma = 0$ and $\beta \neq 0$, then the assumption of $\delta = \varepsilon = 0$ leads to the obvious contradiction of $\beta = 0$. This shows that a coupler satisfying the previously mentioned conditions 1) and 2) can never be perfectly directive. A finite degree of coupling will always exist between the input side port and 1) the center port adjacent to its terminal [for example, between ports 1 and 2 of Fig. 3(b)], and 2) all the other ports [4, 5, and 6 of Fig. 3(b)] of the opposite side.

The matching and coupling conditions of a three-line coupler can be derived from the impedance matrix whose elements are given in Table I. Such a derivation is, however, very tedious and does not provide any physical insight to the problem. The method which will be used in this section is the one which was initially proposed by Jones and Bolljahn [10] and then extended a decade later by Levy [11].

Voltage sources of suitable values as shown in Fig. 3(a) have been considered as being connected to the ports of a three-line coupler; their phase and magnitude relation is such that for each set of sources only one mode can be excited. Additionally, a superposition of all the modes results in a configuration where an input signal of amplitude 1 is connected to one of the side ports of the coupler and all the others are terminated in Z_0 [Fig. 3(b)]. Each line of the coupler can be treated for some particular mode excitation as a two-port network for which the reflection and transmission coefficients are related to its $[ABCD]$ matrix through the following equations [11]:

$$\Gamma = \frac{A + B/Z_0 - CZ_0 - D}{A + B/Z_0 + CZ_0 + D} \tag{IV.8}$$

$$T = \frac{2}{A + B/Z_0 + CZ_0 + D}. \tag{IV.9}$$

By introducing the values of the elements of the $[ABCD]$ matrix into (IV.8) and (IV.9), one obtains the reflection and transmission coefficients of each mode in terms of the corresponding mode impedances and electrical lengths

$$\Gamma_x = \frac{j\left[\frac{Z_x}{Z_0} - \frac{Z_0}{Z_x}\right]\sin\theta_x}{\phi_x} \tag{IV.10}$$

$$T_x = \frac{2}{\phi_x} \tag{IV.11}$$

where $\phi_x = 2\cos\theta_x + j[(Z_x/Z_0) + (Z_0/Z_x)]\sin\theta_x$, and $x = oe, ee, oo$. Using the superposition principle, the total voltages emerging from the ports of the coupler are found to be

$$V_1 = \tfrac{1}{2}\Gamma_{oe} + \frac{1}{2+\mu^2}\Gamma_{ee} + \frac{\mu^2}{2(2+\mu^2)}\Gamma_{oo} \tag{IV.12}$$

$$V_2 = \frac{\mu}{2+\mu^2}[\Gamma_{ee} - \Gamma_{oo}] \tag{IV.13}$$

$$V_3 = -\tfrac{1}{2}\Gamma_{oe} + \frac{1}{2+\mu^2}\Gamma_{ee} + \frac{\mu^2}{2(2+\mu^2)}\Gamma_{oo} \tag{IV.14}$$

$$V_4 = -\tfrac{1}{2}T_{oe} + \frac{\mu}{2+\mu^2}T_{ee} + \frac{\mu^2}{2(2+\mu^2)}T_{oo} \tag{IV.15}$$

$$V_5 = \frac{\mu}{2+\mu^2}[T_{ee} - T_{oo}] \tag{IV.16}$$

$$V_6 = \tfrac{1}{2}T_{oe} + \frac{1}{2+\mu^2}T_{ee} + \frac{\mu^2}{2(2+\mu^2)}T_{oo}. \tag{IV.17}$$

Although the phase velocity is different for each of the three possible modes, the assumption of equal electrical lengths ($\theta_{oe} = \theta_{ee} = \theta_{oo}$) will be made for the following calculations.

One of the major requirements of a three-line coupler is to have matched side ports in the operating frequency band. Equation (IV.12) gives for $V_1 = 0$ and for a quarter-wavelength coupler the matching condition

$$[1 - m][Z_{oe}^2 Z_{ee}^2 Z_{oo}^2 - Z_0^6] + Z_0^2 Z_{oe}^2[Z_{ee}^2 - mZ_{oo}^2] + Z_0^4[mZ_{ee}^2 - Z_{oo}^2] = 0 \quad \text{(IV.18)}$$

with $m = -\mu^2/2$.

If the matching condition $V_1 = 0$ is satisfied, then the coupling coefficient from ports 1–3 [Fig. 3(a)] is

$$V_3 = -\Gamma_{oe}. \quad \text{(IV.19)}$$

Since in practical applications it is usually required to have a perfect isolation between two adjacent side ports, (IV.19) suggests that Γ_{oe} should in such a case be zero or, in other words, that the mode impedance Z_{oe} should be equal to the terminating impedance Z_0

$$Z_0 = Z_{oe}. \quad \text{(IV.20)}$$

The matching condition (IV.18) can be simplified under the condition (IV.20), becoming

$$Z_0^2 = \frac{1}{2}\left[\frac{1+m}{1-m}(Z_{ee}^2 - Z_{oo}^2) + \sqrt{\left(\frac{1+m}{1-m}\right)^2 [Z_{ee}^2 - Z_{oo}^2]^2 + 4Z_{ee}^2 Z_{oo}^2}\right]. \quad \text{(IV.21)}$$

Under the conditions of perfect matching and isolation the coupling from port 1 to port 2 can be evaluated as

$$V_2 = \frac{1}{\mu}\Gamma_{ee}. \quad \text{(IV.22)}$$

It can be seen from (IV.10) and (IV.22) that the maximum value of Γ_{ee} and thus of V_2 occurs for the case of a quarter-wavelength three-line coupler. Equation (IV.22) can therefore be written as

$$V_2 = \frac{1}{\mu}\frac{Z_{ee}^2 - Z_0^2}{Z_{ee}^2 + Z_0^2}. \quad \text{(IV.23)}$$

The coupling coefficients of all the remaining ports are as follows:

$$V_4 = -j\left[-\frac{1}{2} + \frac{Z_{oe}}{2+\mu^2}\frac{2Z_{ee}(Z_{oe}^2 + Z_{oo}^2) + \mu^2 Z_{oo}(Z_{oe}^2 + Z_{ee}^2)}{(Z_{ee}^2 + Z_{oe}^2)(Z_{oo}^2 + Z_{oe}^2)}\right] \quad \text{(IV.24)}$$

$$V_5 = -j\frac{2}{2+\mu^2}\frac{Z_{oo}Z_{ee} + Z_{oe}^2}{(Z_{ee}^2 + Z_{oe}^2)(Z_{oo}^2 + Z_{oe}^2)} Z_{oe}(Z_{ee} - Z_{oo}) \quad \text{(IV.25)}$$

$$V_6 = -j\left[\frac{1}{2} + \frac{Z_{oe}}{\mu^2}\frac{2Z_{ee}(Z_{oe}^2 + Z_{oo}^2) + \mu^2 Z_{oo}(Z_{oe}^2 + Z_{ee}^2)}{(Z_{ee}^2 + Z_{oe}^2)(Z_{oo}^2 + Z_{oe}^2)}\right]. \quad \text{(IV.26)}$$

V. The Model Used for the Numerical Analysis of the Three-Line Coupler

In this part of the paper, the dependence of the characteristic mode impedances on the geometry of the coupler will be derived by the aid of a digital computer.

Several methods exist for the computation of the characteristic impedance of single- or multiple-conductor lines. Yamashita and Mittra [13] have proposed the use of integral equations calculated with the aid of Green's functions. Gupta [12] uses the electrostatic- and magnetostatic-energy integrals in order to calculate a lower and an upper bound of the impedance; the resulting impedance values are therefore very accurate because they are based on the average value of the aforementioned bounds. Itakura *et al.* [4] used a conformal mapping technique in order to derive exact solutions for a structure consisting of three parallel conductors in a homogeneous medium. Conformal mapping techniques give, however, only approximate solutions for inhomogeneous media. The method adopted for our derivations was a finite-difference numerical solution of Laplace's equation $\nabla^2\psi = 0$ in a two-dimensional space and the use of Gauss law for the calculations thereafter. The wave propagation along the three lines has been assumed to be a pure TEM one and the lines were enclosed in a shielding box.

It is known that the impedance matrix of a coupler can be written as

$$[z]^2 = \frac{1}{c^2}[c_{\text{air}}]^{-1}[c_{\text{dielectric}}]^{-1} \quad \text{(V.1)}$$

where $[c_{\text{dielectric}}]$ and $[c_{\text{air}}]$ are the static capacitance matrices of the structure with and without an air–dielectric interface. The evaluation of the previously given capacitance matrices allows the calculation of the elements z_{ij}, $(i,j = 1,2,3)$ of the impedance matrix and, consequently, a knowledge of the mode impedances Z_{oe}, Z_{ee}, and Z_{oo}.

The model which has been used for the numerical analysis is shown in Fig. 4; two grids, a main one and a finer one in the vicinity of the lines, have been used because of accuracy considerations. The potential at each of the nodes is calculated using the five-point formula which is known to give an error of the order of h^2 (where h is the distance between two successive nodes). A better accuracy is, of course, expected in theory by the use of the nine-point formula, but in practice [14] the five-point formula seems superior because of the existing reentrant corners where a singularity of the electric field exists.

The execution of the developed finite-difference program is continued until an accuracy of 10^{-4} is achieved. Then the charge associated with each conductor is evaluated by integrating around it. Because of the boundary between the main and the fine grid of Fig. 4, it was necessary to derive some special finite-difference formulas for certain nodes of the grid. The optimum over relaxation factor β has been

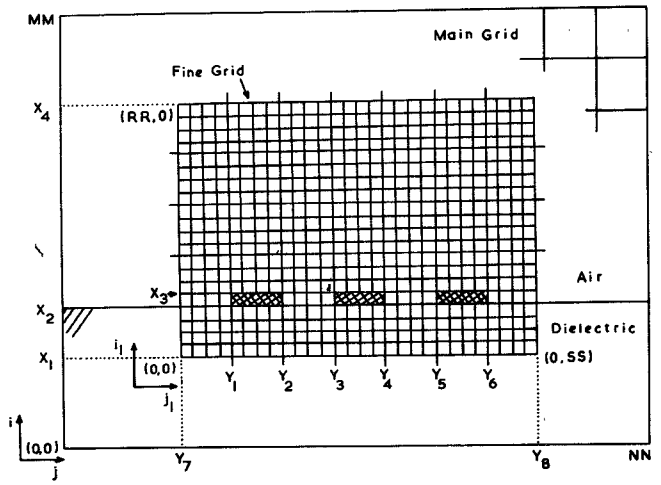

Fig. 4. The model used for the numerical analysis of a shielded three-line microstrip coupler.

evaluated by examining the number of iterations which were necessary for the convergence of the solution and it has been found that $\beta_{opt} = 1.85$. The accuracy of the program has been checked by eliminating one of the three lines and comparing the obtained results with those by Bryant and Weiss [15] for a two-line coupler; the values of mode impedances obtained by our program were never different by more than 2 percent from those of Bryant.

The evaluation of the mode impedances can be done by using (V.1) and (II.4)–(II.6). Such a calculation does, however, need the use of a computer because of the numerous algebraic equations resulting from (V.1). A less complicated solution can be obtained by substituting the mode-capacitance values of (II.19)–(II.21) into the following formula:

$$Z_x = \frac{1}{c\sqrt{C_{x,\text{air}} C_{x,\text{diel}}}} \tag{V.2}$$

where Z_x, ($x = oe,ee,oo$) are the mode impedances, c is the free-space velocity and $C_{x,\text{diel}}, C_{x,\text{air}}$ are the mode capacitances in the presence of a dielectric substrate ($k > 1$) and without it ($k = 1$), respectively. The effective dielectric constant $k_{\text{eff},x}$, the velocity v_x, and the normalized wavelength λ_x/λ_0 of the modes propagating in microstrip three-conductor systems are given by

$$\sqrt{\frac{C_{x,\text{air}}}{C_{x,\text{diel}}}} = \frac{1}{\sqrt{k_{\text{eff},x}}} = \frac{v_x}{c} = \frac{\lambda_x}{\lambda_0} \tag{V.3}$$

where c and λ_0 are the free-space velocity and wavelength, respectively.

VI. Mode-Impedance Charts and Synthesis of a Three-Line Coupler

The analyzed shielded microstrip coupler has been considered as having three lines of equal width w and separation s. The height of the dielectric alumina substrate ($k = 9.8$) will in the following be symbolized by h. Using the developed program for the three-line coupler, the mode impedances Z_{oe}, Z_{ee}, and Z_{oo} have been computed for various w/h and s/h ratios. Most of the results have been obtained for infinitely thin microstrip lines, but an investigation of the finite thickness effect has also been undertaken.

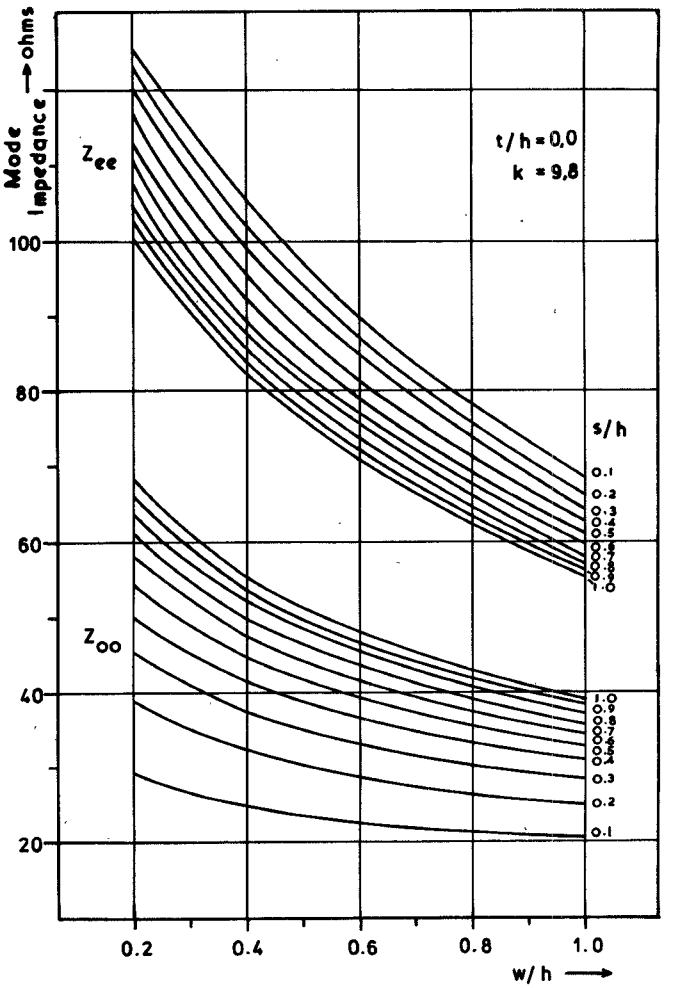

Fig. 5. The dependence of the mode impedances Z_{ee} and Z_{oo} on the w/h and s/h ratio for a three-line microstrip coupler ($k = 9.8$, $t/h = 0$), where w, s, and t are the width, separation, and thickness of the lines, and h is the substrate thickness.

Figs. 5 and 6 show the mode-impedance dependence on the geometry, w/h and s/h, of the coupler; for applications where a more accurate design is needed, the results have also been tabulated[1] together with the mode capacitances $C_{x,\text{air}}$ and $C_{x,\text{diel}}$, ($x = oe,ee,oo$) for the case of air only ($k = 1$) and for the case of an air–dielectric interface ($k = 9.8$), respectively. The effective dielectric constant $k_{\text{eff},x}$ and the mode phase velocity v_x can also be found in these tables.

Fig. 7 shows the reduction of the mode impedances due to the finite thickness t of the microstrip lines. The maximum change of impedance is of the order of 8 Ω for a ratio $t/h = 0.1$. Since in most microwave applications the t/h ratio is usually not more than 0.01, the thickness effect has been considered as being very small and has therefore not been explored extensively.

[1] Within the space provided by a paper, it is not possible to include these tables here. However, they can be obtained from the authors on request.

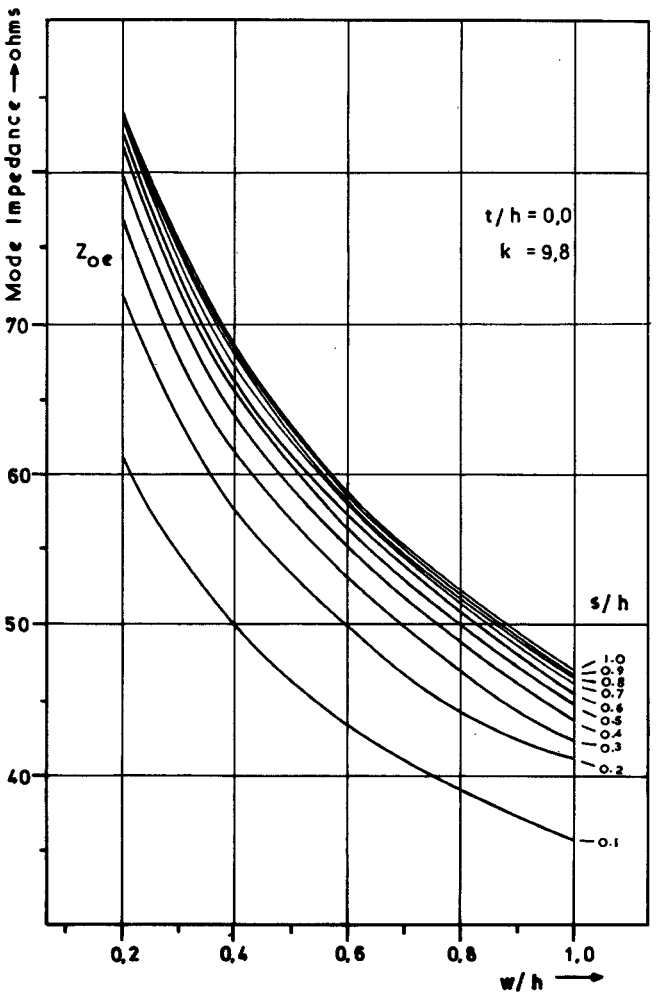

Fig. 6. The dependence of the mode impedance Z_{oe} on the w/h and s/h ratio for a three-line microstrip coupler ($k = 9.8$, $t/h = 0$) where w, s, and t are the width, separation, and thickness of the lines, and h is the substrate thickness.

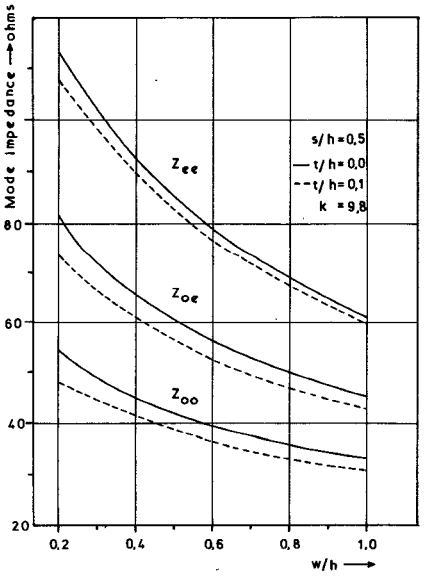

Fig. 7. Comparison of a finite ($t/h = 0.1$) and of a zero thickness ($t/h = 0$) three-line microstrip coupler.

The effective wavelength λ_x for each of the three possible modes can be found from a knowledge of the effective dielectric constant for a particular coupler geometry. In practice, the length of the coupling region of a quarter-wavelength coupler can be evaluated using the following formula:

$$l = \tfrac{1}{4}\lambda = \tfrac{1}{4}[\lambda_{oo}\lambda_{ee}\lambda_{oe}]^{1/3} \qquad \text{(VI.1)}$$

where the λ_x, ($x = oo,ee,oe$) correspond to the wavelengths of each of the modes.

It is interesting to note that for a given w/h ratio the phase velocity is generally increased by decreasing the s/h value, but the overall change is larger in the case of the oe and ee modes than for the oo one.

The synthesis procedure of a three-line coupler can in conclusion be summarized as follows.

1) Determination of the desired degree of coupling and terminating impedance $Z_0 = Z_{oe}$ and calculation of the necessary mode impedances Z_{ee} and Z_{oo} by solving (IV.21) and (IV.23).

2) Evaluation of the required coupler geometry from Figs. 5 and 6.

3) Calculation of the length of the coupling region by evaluating the effective wavelengths for each mode and using (VI.1).

VII. Experiment: Fabrication and Test of a Three-Line Coupler

A three-line coupler has been manufactured and tested in order to verify the theory presented in the previous sections of the paper. The terminating impedance of all ports was 50 Ω and the coupling coefficient from a side port to the main center line has been chosen to be 10 dB. These requirements result in the following combination of mode impedances for an alumina substrate of $k = 9.8$: $Z_{ee} = 78.4\,\Omega$ and $Z_{oo} = 30.0\,\Omega$. The necessary geometrical configuration should thus be $w/h = 0.68$ and $s/h = 0.3$; this requires for a 635-μm-thick substrate a separation of the lines by 190.5 μm. By evaluating the effective dielectric constant for each mode and from there the corresponding effective wavelengths, the length of the coupling region could be determined as 7.69 mm for a quarter-wavelength coupler with a midband frequency at 4 GHz. A special brass mount was constructed and a carefully designed coaxial-to-microstrip transition used throughout the experiments. The input reflection coefficient could be considerably improved by gradually transforming the cylindrical inner conductor of the OSM-connector at the transition side into a triangular shape and by avoiding any gap between the ground plane of the alumina substrate and that of the OSM-connector. After evaporation of a 200-Å Cr layer and a 1000-Å Au layer and the use of the floatoff method with Shipley photoresist, conventional gold-plating techniques were used for the fabrication of the three-line coupler on alumina substrates. The final thickness of the Au line was 5 μm. The substrate thickness was 635 μm showing negligibly small surface variations. The lines deposited on the substrates by the floatoff method have sharp edges since the

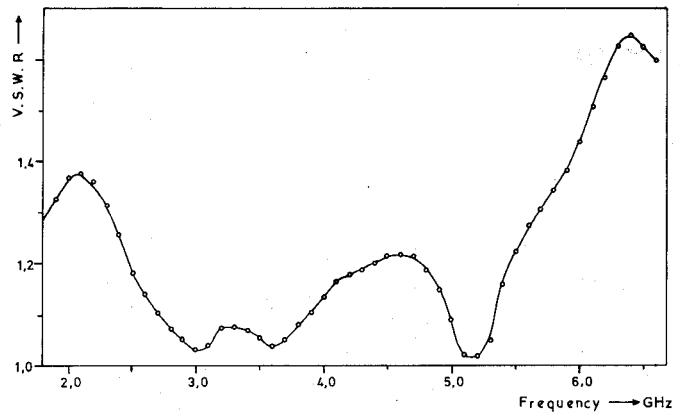

Fig. 8. Typical frequency dependence of the VSWR for a side input port of an experimental three-line coupler.

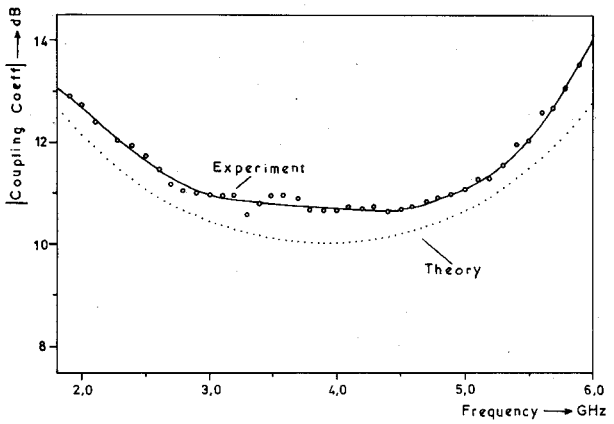

Fig. 9. Typical frequency dependence of the coupling from a side port to the center line of a 10-dB three-line coupler.

quality of this fabrication process is primarily limited by the optical properties of the photoresist rather than a chemical etching of large gold surfaces.

The VSWR and the coupling from one side port to the adjacent port of the main line have been measured using an HP network analyzer, and the results are shown in Figs. 8 and 9 for the frequency range of 1.8–6.5 GHz. It can be seen that the VSWR changes in the frequency range of 3–5 GHz from a minimum value of 1.03 to a maximum one of 1.18. This result has been considered to be in good agreement with the intended matching of the input ports. The average coupling coefficient for the aforementioned frequency band is typically of the order of 10.8 dB. There is therefore a 0.8-dB deviation from the theoretically predicted coupling value which is mainly due to the assumptions of our theory such as is given by (IV.1), but also due to other effects as, for example, the existence of losses in the structure.

The isolation characteristics of the side ports have also been examined and found to vary between 21 and 26 dB in the operating frequency range of 3–5 GHz. This was again in good agreement with the theoretical predictions of good isolation.

Finally, a photograph of the constructed 10-dB three-line coupler is given in Fig. 10.

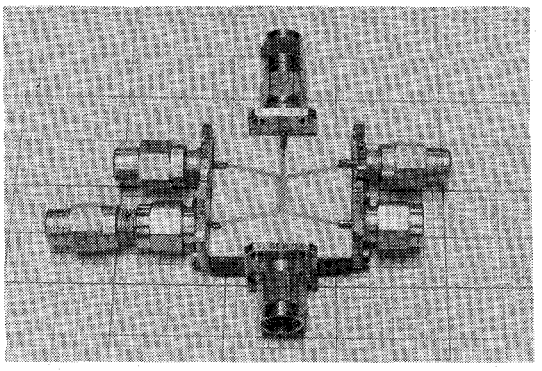

Fig. 10. Photograph of an experimental 10-dB three-line coupler.

VIII. Conclusions

The fundamental modes of propagation have been derived for an array of three parallel conductors. The properties of such a network have been examined by the use of only three mode impedances which are the same for both center and side conductors.

It has been shown both theoretically and experimentally that it is possible to realize three-line couplers having:

1) perfectly matched input side ports;
2) a finite controllable value of coupling between any side port and the center line;
3) perfect isolation between any two side ports at either end of the lines.

These couplers are particularly useful in communications applications where it is often necessary to combine two signals into one without any interaction of the signal sources. Although there is a disagreement of 0.8 dB between the predicted and the experimentally evaluated value of coupling coefficients for a 10-dB coupler, the developed theory can be considered satisfactory for most microwave applications.

Acknowledgment

The authors wish to thank Prof. H. Hasegawa for his helpful discussions concerning the coupler analysis and Dr. K. Tomizawa for his constructive suggestions during the development of the finite-difference program. They also wish to thank Prof. H. Beneking and, in particular, W. Nievendick at the TH-Aachen, Germany, who introduced one of us (D.P.) to the technological aspects of microstrip structures during his stay at the Institut für Halbleitertechnik.

References

[1] G. L. Matthaei, "Interdigital band-pass filters," *IEEE Trans. Microwave Theory Tech.*, vol. MTT-10, pp. 479–491, November 1962.
[2] E. G. Cristal, "Coupled circular cylindrical rods between parallel ground planes," *IEEE Trans. Microwave Theory Tech.*, vol. MTT-12, pp. 428–439, July 1964.
[3] W. P. Ou, "Design equations for an interdigitated directional coupler," *IEEE Trans. Microwave Theory Tech.*, vol. MTT-21, pp. 253–255, February 1975.
[4] Y. Itakura, T. Azakami, and S. Yamamoto, "Coupled strip transmission line with three center conductors," presented at the

1965 Microwave Transmission System Conference of the Institute of Electr. Commun. Eng. of Japan.
[5] S. Yamamoto, T. Azakami, and K. Itakura, "Coupled strip transmission line with three center conductors," *IEEE Trans. Microwave Theory Tech.*, vol. MTT-14, pp. 446–461, October 1966.
[6] H. Uchida, *Fundamentals of Coupled Lines and Multiwire Antennas.* Sendai, Japan: Sasaki Printing and Publishing Company Limited, 1967.
[7] D. Pavlidis and H. L. Hartnagel, "A microwave P.S.K. pulse modulator," *AEÜ*, vol. 27, no. 10, pp. 450–451, October 1973.
[8] D. Pavlidis, H. L. Hartnagel, and K. Tomizawa, "Phase transients of injection locked Gunn oscillators for microwave pulse communication," in *Proceedings of the 4th European Microwave Conference* (Montreux, Switzerland), September 1974, pp. 318–322.
[9] R. E. Collin, *Field Theory of Guided Waves.* New York: McGraw-Hill Book Company Inc., 1960, Ch. 4.
[10] E. M. T. Jones and J. T. Bolljahn, "Coupled-strip transmission-line filters and directional couplers," *IRE Trans. Microwave Theory Tech.*, vol. MTT-4, pp. 75–81, 1956.
[11] R. Levy, "Transmission-line directional couplers for very broad-band operation," *Proc. IEE*, vol. 112, no. 3, pp. 469–476, 1965.
[12] R. R. Gupta, "Accurate impedance determination of coupled TEM conductors," *IEEE Trans. Microwave Theory Tech.*, vol. MTT-17, pp. 479–489, 1969.
[13] E. Yamashita and R. Mittra, "Variational method for the analysis of microstrip lines," *IEEE Trans. Microwave Theory Tech.*, vol. MTT-16, pp. 251–256, April 1968.
[14] J. W. Duncan, "The accuracy of finite difference solutions of Laplace's equations," *IEEE Trans. Microwave Theory Tech.*, vol. MTT-15, pp. 575–582, October 1967.
[15] T. G. Bryant and J. A. Weiss, "Tables with parameters for microstrip lines," Document No. NAPS-0087, ADI Auxiliary Publications Service, American Society of Information Sciences, New York.

General TE_{011}-Mode Waveguide Bandpass Filters

ALI E. ATIA, MEMBER, IEEE, AND ALBERT E. WILLIAMS, MEMBER, IEEE

Abstract—**A new structure for high-Q TE_{011}-mode circular waveguide cavities is introduced and shown to realize the most general bandpass-filter transfer functions. Methods of improving the mode purity and suppressing the degenerate TM_{111} mode are presented. Several experimental narrow-bandpass filters having finite attenuation poles have been constructed; their measured responses show excellent agreement with theory. Average realizable unloaded Q's of 20 000 and 16 000 have been achieved at 8 and 12 GHz, respectively.**

INTRODUCTION

MANY modern microwave communications-system applications require exacting filter specifications in terms of selectivity, midband insertion loss, gain slope, and group delay. Synthesis methods have been developed for the realization of general transfer functions in multiple-coupled cavities [1]. Successful implementations of these synthesis techniques have been demonstrated by constructing narrow-bandpass waveguide filters in dual-mode circular cavities [2], dual-mode square cavities, and single-mode rectangular cavities [3] excited in dual TE_{111}, dual TE_{101}, and single TE_{101} modes, respectively.

The gain slope and midband insertion losses of bandpass filters are closely related to the practically realizable unloaded Q's of the cavities and the fractional bandwidth of the filters. At high frequencies (centimeter through millimeter wave), the achievable unloaded Q of waveguide cavities excited in the fundamental modes can be a limiting factor in the realization of highly selective narrow-bandpass filters having small gain slopes and in-band insertion losses. Furthermore, in high-power multiplexing applications it is important to minimize the filter losses. Typically, silver-plated waveguide-cavity filters excited in the fundamental mode can be realized with average unloaded Q's of about 10 000 at S band. At higher frequencies, lower unloaded Q's are realized due to the $1/\sqrt{f}$ dependence. For example, Q's ranging from 7000 to 5500 are achieved at X band.

An obvious way of obtaining a higher unloaded Q is to employ a higher order cavity mode, although care must be taken to ensure satisfactory cavity tuning control and suppression of adjacent modes. One mode which has been successfully employed is the circular TE_{011} mode. Known realizations of this mode are cascaded (direct-coupled) structures [4] which limit the class of transfer functions that can be realized to all-pole functions (e.g., Chebychev and Butterworth). More general characteristics, e.g., functions possessing transmission zeros at finite frequencies and nonminimum phase functions, cannot be realized in these simple direct-coupled structures.

This paper demonstrates the realization of the most general filter transfer functions in waveguide structures excited in the high-Q TE_{011} mode. It is well known that this can only be achieved if couplings among certain non-cascaded cavities are realized with arbitrary signs. A new structure satisfying the canonical form of multiple-coupled cavity realization [1] is introduced.

One of the difficulties encountered in the utilization of the TE_{011} circular waveguide-cavity mode for filter realization is the presence of the degenerate TM_{111} mode. Methods of splitting the degeneracy of the two modes are presented,

Manuscript received January 15, 1976; revised April 5, 1976. This paper is based upon work performed in COMSAT Laboratories under the sponsorship of the Communications Satellite Corporation.
The authors are with the COMSAT Laboratories, Clarksburg, MD 20734.